Supporting Information

On the Ligand Promiscuity between the Efflux Pumps Human P-Glycoprotein and *S. aureus* NorA

Jean Pierre Brincat,[a] Fabio Broccatelli,[a] Stefano Sabatini,[b] Maria Frosini,[c] Annalisa Neri,[c] Glenn W. Kaatz,[d] Gabriele Cruciani,[a] Emanuele Carosati[a]*

[a]Dipartimento di Chimica, Università degli Studi di Perugia, and [b]Dipartimento di Chimica e Tecnologia del Farmaco, Università degli Studi di Perugia, 06123 Perugia, Italy, [c] Department of Neuroscience, Pharmacology Unit, University of Siena, Siena, Italy, [d]Department of Internal Medicine, Division of Infectious Diseases, School of Medicine, Wayne State University and the John D. Dingell Department of Veterans Affairs Medical Center, Detroit, Michigan 48201 USA

* corresponding author: emanuele@chemiome.chm.unipg.it

Table of Contents:

Table S1. Structures of Dataset Compounds

Table denoting the code (as it appears in the main text), chemical structure, SMILES code and Polar Capacity at -3.0 kcal mol^{-1} of all the compounds listed in Table 1 of the article.

ID	Structure	SMILES Code	Polar Capacity at -3.0 kcal mol^{-1}
1	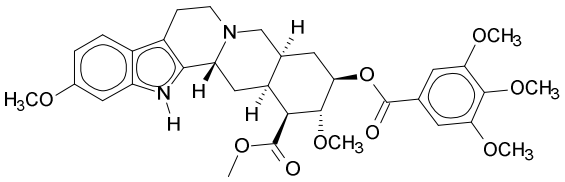	O=C(OC1CC2CN3CCc4c5ccc(OC)cc5nc4C3CC2C(C(=O)OC)C1OC)c6cc(OC)c(OC)c(OC)c6	0.12
2	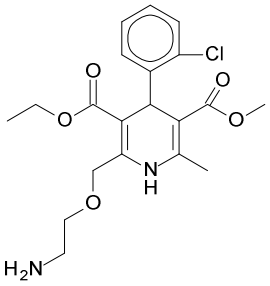	CCOC(=O)C1=C(NC(=C(C1C2=CC=CC=C2Cl)C(=O)OC)C)COCCN	0.20
3	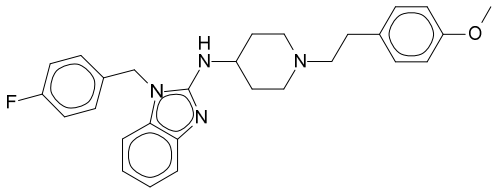	COC1=CC=C(C=C1)CCN2CCC(CC2)NC3=NC4=CC=CC=C4N3CC5=CC=C(C=C5)F	0.08
4	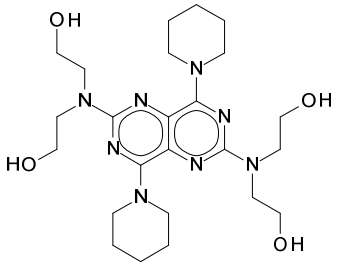	C1CCN(CC1)C2=NC(=NC3=C2N=C(N=C3N4CCCCC4)N(CCO)CCO)N(CCO)CCO	0.26
5	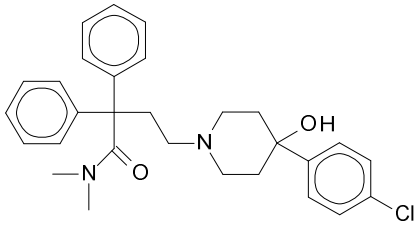	CN(C)C(=O)C(CCN1CCC(CC1)(C2=CC=C(C=C2)Cl)O)(C3=CC=CC=C3)C4=CC=CC=C4	0.09

6	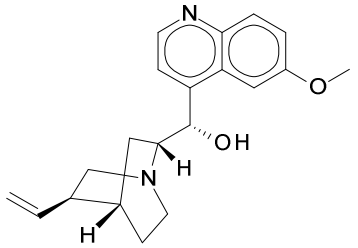	COC1=CC2=C(C=CN=C2C=C1)[C@@H]([C@H]3C[C@@H]4CCN3C[C@@H]4C=C)O	0.13
7	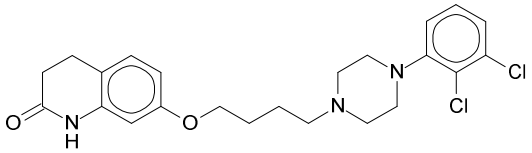	C1CC(=O)NC2=C1C=CC(=C2)OCCCCN3CCN(CC3)C4=C(C(=CC=C4)Cl)Cl	0.19
8	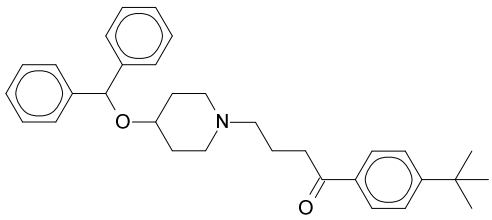	CC(C)(C)C1=CC=C(C=C1)C(=O)CCCN2CCC(CC2)OC(C3=CC=CC=C3)C4=CC=CC=C4	0.07
9	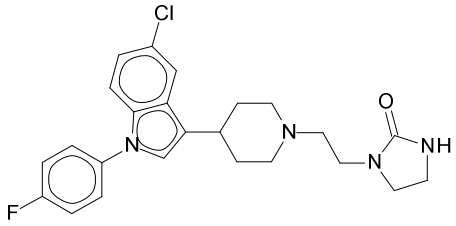	C1CN(CCC1C2=CN(C3=C2C=C(C=C3)Cl)C4=CC=C(C=C4)F)CCN5CCNC5=O	0.13
10	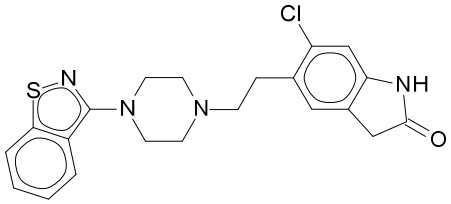	C1CN(CCN1CCC2=C(C=C3C(=C2)CC(=O)N3)Cl)C4=NSC5=CC=CC=C54	0.15
11	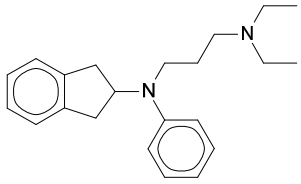	CCN(CC)CCCN(C1CC2=CC=CC=C2C1)C3=CC=CC=C3	0.02
12	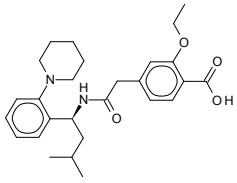	CCOC1=C(C=CC(=C1)CC(=O)N[C@@H](CC(C)C)C2=CC=CC=C2N3CCCCC3)C(=O)O	0.12

13	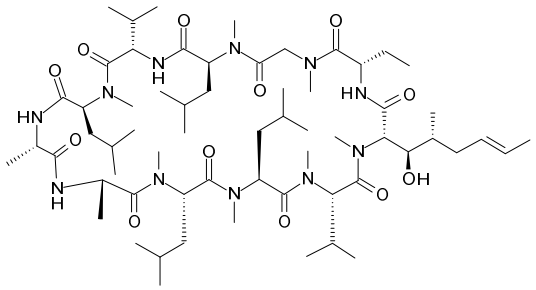	CC[C@H]1C(=O)N(CC(=O)N([C@H](C(=O)N[C@H](C(=O)N([C@H](C(=O)N[C@H](C(=O)N[C@@H](C(=O)N([C@H](C(=O)N([C@H](C(=O)N([C@H](C(=O)N1)[C@@H]([C@H](C)C/C=C/C)O)C)C(C)C)CC(C)C)C)CC(C)C)C)C)CC(C)C)C)C(C)C)CC(C)C)C	0.22
14	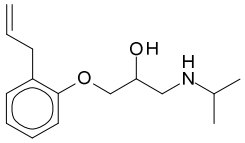	CC(C)NCC(COC1=CC=CC=C1CC=C)O	0.12
15	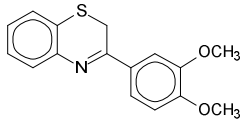	COc1ccc(cc1OC)C2=Nc3ccccc3SC2	0.05
16	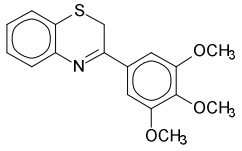	COc1cc(cc(OC)c1OC)C2=Nc3ccccc3SC2	0.05
17	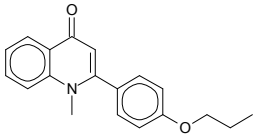	O=C1C=C(N(C)c2ccccc12)c3ccc(OCCC)cc3	0.10
18	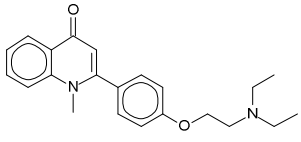	C1(=CC(=O)c2ccccc2N1C)c3ccc(cc3)OCCN(CC)CC	0.10
19	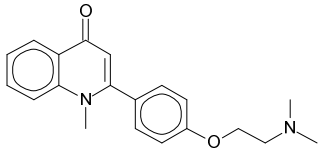	C1(=CC(=O)c2ccccc2N1C)c3ccc(cc3)OCCN(C)C	0.13
20	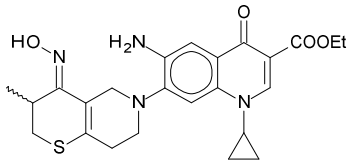	CCOC(=O)c1cn(c2cc(c(cc2c1=O)N)N3CCC4=C(C3)/C(=N/O)/C(CS4)C)C5CC5	0.18

21	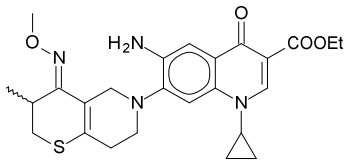	CCOC(=O)c1cn(c2cc(c(cc2c1=O)N)N3CCC4=C(C3)/C(=N/OC)/C(CS4)C)C5CC5	0.14
22	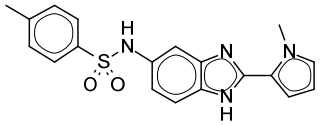	Cc1ccc(cc1)S(=O)(=O)Nc2ccc3c(c2)nc([nH]3)c4ccccn4C	0.11
23	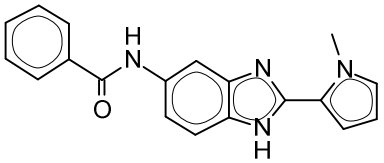	Cn1cccc1c2[nH]c3ccc(cc3n2)NC(=O)c4ccccc4	0.10
24	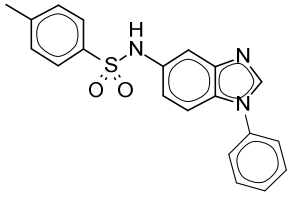	Cc1ccc(cc1)S(=O)(=O)Nc2ccc3c(c2)ncn3c4ccccc4	0.14
25	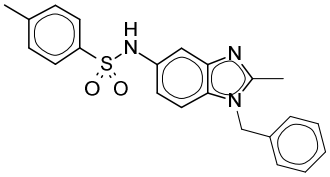	Cc1ccc(cc1)S(=O)(=O)Nc2ccc3c(c2)nc(n3Cc4ccccc4)C	0.11
26	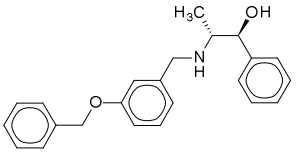	C[C@H]([C@H](c1ccccc1)O)NCc2cccc(c2)OCc3ccccc3	0.08
27	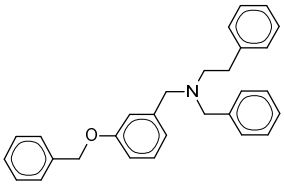	c1ccc(cc1)CCN(Cc2ccccc2)Cc3cccc(c3)OCc4ccccc4	0.02
28	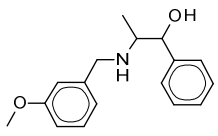	CC(C(c1ccccc1)O)NCc2cccc(c2)OC	0.10

29	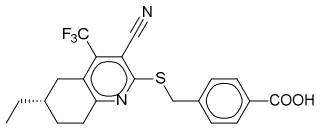	CC[C@H]1CCc2c(c(c(c(n2)SCc3ccc(cc3)C(=O)O)C#N)C(F)(F)F)C1	0.27
30	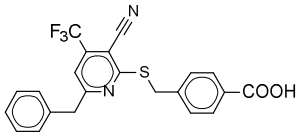	c1ccc(cc1)Cc2cc(c(c(n2)SCc3ccc(cc3)C(=O)O)C#N)C(F)(F)F	0.26
31	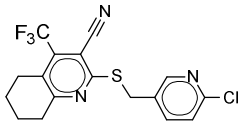	c1cc(ncc1CSc2c(c(c3c(n2)CCCC3)C(F)(F)F)C#N)Cl	0.22
32	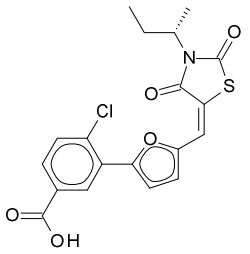	CC[C@H](C)N1C(=O)/C(=C\c2ccc(o2)c3cc(ccc3Cl)C(=O)O)/SC1=O	0.20
33	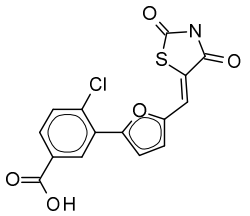	c1cc(c(cc1C(=O)O)c2ccc(o2)/C=C\3/C(=O)NC(=O)S3)Cl	0.35
34	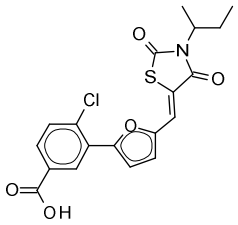	CCC(C)N1C(=O)/C(=C/c2ccc(o2)c3cc(ccc3Cl)C(=O)O)/SC1=O	0.24
35	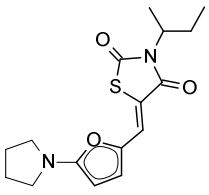	CCC(C)N1C(=O)/C(=C/c2ccc(o2)N3CCCC3)/SC1=O	0.15

Table S2. Common Names and IUPAC Names

Table denoting the code (as it appears in the main text) and the common name or IUPAC name of all the compounds listed in Table 1 of the article.

Number	Common Name or IUPAC Name
1	Reserpine
2	Amlodipine
3	Astemizole
4	Dipyridamole
5	Loperamide
6	Quinidine
7	Aripiprazole
8	Ebastine
9	Sertindole
10	Ziprasidone
11	Aprindine
12	Repaglinide
13	Cyclosporine A
14	Alprenolol
15	3-(3,4-dimethoxyphenyl)-2H-1,4-benzothiazine
16	3-(3,4,5-trimethoxyphenyl)-2H-1,4-benzothiazine
17	1-methyl-2-(4-propoxyphenyl)quinolin-4-one
18	2-[4-(2-diethylaminoethyloxy)phenyl]-1-methyl-quinolin-4-one
19	2-[4-(2-dimethylaminoethyloxy)phenyl]-1-methyl-quinolin-4-one
20	ethyl 6-amino-1-cyclopropyl-7-[(4E)-4-hydroxyimino-3-methyl-3,5,7,8-tetrahydro-2H-thiopyrano[3,2-c]pyridin-6-yl]-4-oxo-quinoline-3-carboxylate
21	ethyl 6-amino-1-cyclopropyl-7-[(4E)-4-methoxyimino-3-methyl-3,5,7,8-tetrahydro-2H-thiopyrano[3,2-c]pyridin-6-yl]-4-oxo-quinoline-3-carboxylate

22	4-methyl-N-[2-(1-methylpyrrol-2-yl)-1H-benzimidazol-5-yl]benzenesulfonamide
23	N-[2-(1-methylpyrrol-2-yl)-1H-benzimidazol-5-yl]benzamide
24	4-methyl-N-(1-phenylbenzimidazol-5-yl)benzenesulfonamide
25	N-(1-benzyl-2-methyl-benzimidazol-5-yl)-4-methyl-benzenesulfonamide
26	(1S,2R)-2-[(3-benzyloxyphenyl)methylamino]-1-phenyl-propan-1-ol
27	N-benzyl-N-[(3-benzyloxyphenyl)methyl]-2-phenyl-ethanamine
28	2-[(3-methoxyphenyl)methylamino]-1-phenyl-propan-1-ol
29	4-[[(6S)-3-cyano-6-ethyl-4-(trifluoromethyl)-5,6,7,8-tetrahydroquinolin-2-yl]sulfanylmethyl]benzoic acid
30	4-[[6-benzyl-3-cyano-4-(trifluoromethyl)-2-pyridyl]sulfanylmethyl]benzoic acid
31	2-[(6-chloro-3-pyridyl)methylsulfanyl]-4-(trifluoromethyl)-5,6,7,8-tetrahydroquinoline-3-carbonitrile
32	4-chloro-3-[5-[(E)-[3-[(1S)-1-methylpropyl]-2,4-dioxo-thiazolidin-5-ylidene]methyl]-2-furyl]benzoic acid
33	4-chloro-3-[5-[(Z)-(2,4-dioxothiazolidin-5-ylidene)methyl]-2-furyl]benzoic acid
34	4-chloro-3-[5-[(Z)-(2,4-dioxo-3-sec-butyl-thiazolidin-5-ylidene)methyl]-2-furyl]benzoic acid
35	(5Z)-5-[(5-pyrrolidin-1-yl-2-furyl)methylene]-3-sec-butyl-thiazolidine-2,4-dione

Table S3. Scores and Loading Plots of the VolSurf+ PCA

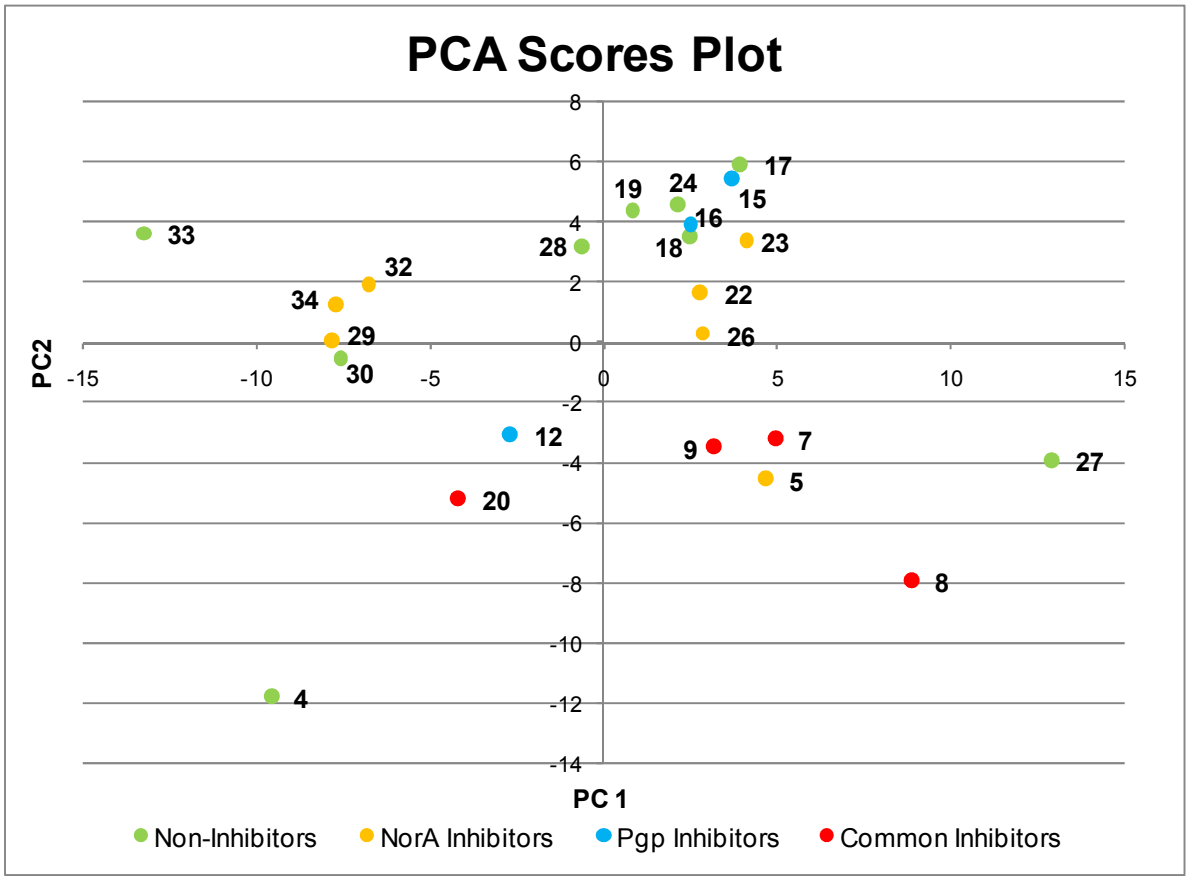

Figure S1. The Scores Plot of the PCA model. The compounds which were found to inhibit both Pgp and NorA ("Common Inhibitors", shown as red points in the graph) have a tendency towards the lower area of the graph (negative PC2). The Loadings Plot (Figure S2) shows that these molecules tend to have high Molecular Weights and large Volumes. Compounds **4** and **27** seem to be false positives, however these can be excluded since the former is too hydrophilic, while the latter lacks polar features. The group of compounds **29**, **32** and **34** in the negative PC1 range seems to indicate that molecules which are more hydrophilic have a tendency to inhibit NorA but not Pgp. Compounds **15** and **16**, due to their benzothiazine structure, might be non-competitive inhibitors of Pgp.

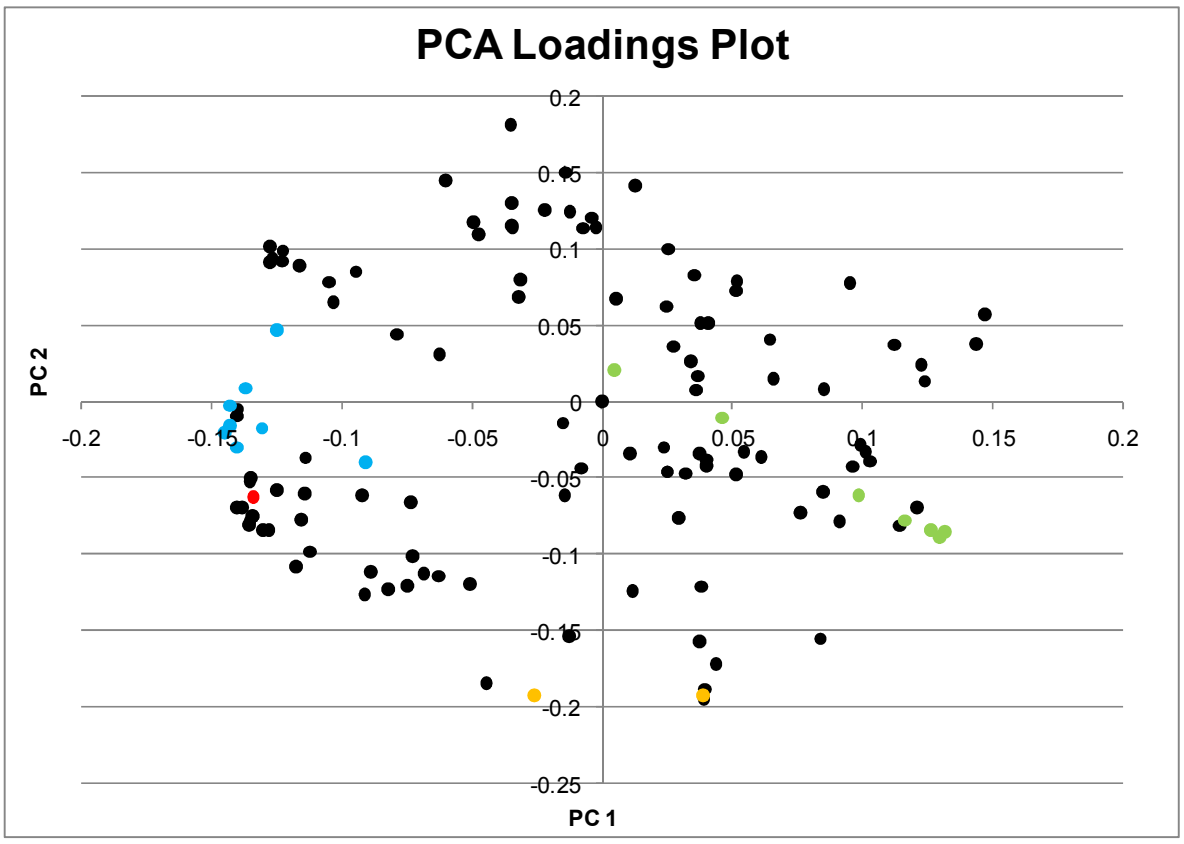

Figure S2. The Loadings Plot of the PCA model. Molecular Weight and Volume are colored yellow, Polar Surface Area (PSA) is colored red, LogD values (the computed partition coefficient between *n*-octanol and water at different pH values) are colored green, and Capacity factors (ratio of hydrophilic volume to the total surface area at eight different GRID energy levels) are colored blue.

Table S4. Detailed Graphical Comparison of NorA and Pgp Inhibitors

Name	Structure	CW1	CW2	CW3	CW4	CW5	CW6	CW7	CW8	PSA
Biricodar	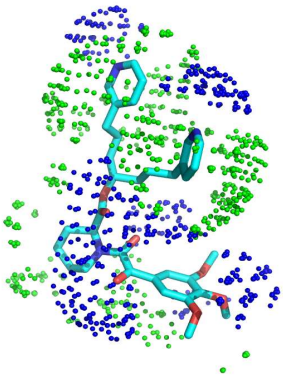	2.28	1.47	0.85	0.37	0.18	0.08	0.03	0.01	123
Elacridar	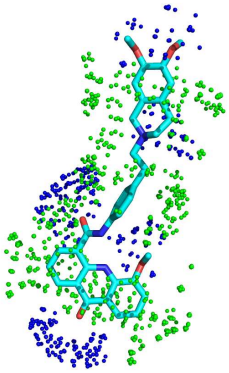	2.35	1.41	0.75	0.29	0.14	0.06	0.02	0.00	95.73
Tariquidar	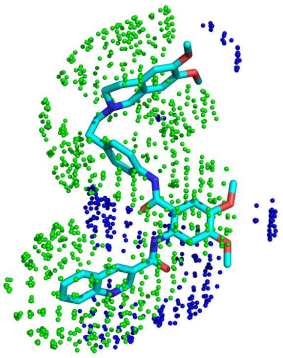	2.22	1.29	0.67	0.25	0.12	0.05	0.02	0.00	119.79
Timcodar	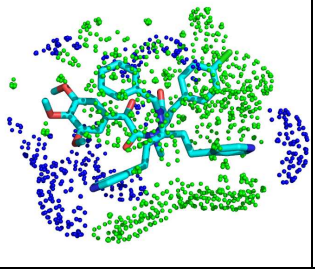	2.29	1.42	0.72	0.29	0.14	0.07	0.03	0.00	116.78

8	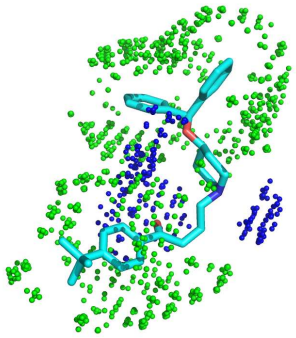	2.06	0.94	0.40	0.14	0.069	0.04	0.01	0.00	32.84
12	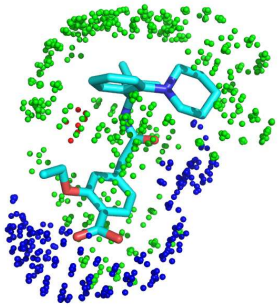	2.10	1.08	0.53	0.22	0.12	0.06	0.03	0.01	80.84
34	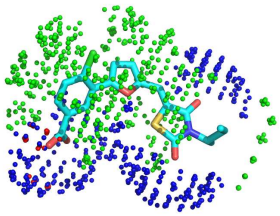	2.45	1.58	0.95	0.45	0.24	0.12	0.05	0.01	99.36

Table S5. Detailed Experimental Methods

1 NorA experiments

1.1 Bacterial Strains

The strain of *S. aureus* employed was SA-1199B, which overexpresses *norA* and also possesses an A116E GrlA substitution.[S1,S2]

1.2 Microbiologic Procedures

MICs were determined in duplicate by microdilution techniques according to CLSI guidelines.[S3,S4]

1.3 EtBr Efflux

The loss of EtBr from *S. aureus* SA-1199B was determined fluorometrically as previously described.[S5] Experiments were performed in duplicate, and the results were expressed as the mean total efflux over a 5 min time course. EtBr efflux of SA-1199B in the presence of test compounds was compared to that determined in their absence and percent reduction in efflux was calculated. The effect of increasing concentrations of test compounds on EtBr efflux was determined to generate dose-response profiles.

2. Pgp experiments

2.1 Cells line and cultures

The L5178Y mouse T-lymphoma cell line transfected with a recombinant MDR1/A retroviral vector (pHa MDR1/A), a generous gift from Dr. Michael M. Gottesman (National Cancer Institute, Bethesda, MD, USA), was used. Human MDR1-expressing cells were selected by culturing the transfected cells with 60 ng/ml colchicine to maintain the expression of the MDR phenotype.[S6] The L5178 MDR1 cell line was grown in McCoy's 5A

medium supplemented with 10% heat-inactivated horse serum, 2 mM L-glutamine, 100 UI/ml penicillin and 0.01 mg/ml streptomycin. Cells were maintained in a humidified incubator with an atmosphere of 95% air and 5% CO_2 at 37 °C. When the cells reached confluency, they were harvested and plated for subsequent passages (up to 20) and for drug treatment. Cultures were initiated at a density of $2x10^5$ cells/ml and grown exponentially to about $2x10^6$ cells/ml in 48h. Cells will were counted in a Burker cytometer before use and their viability tested by Trypan Blue exclusion.

2.2 Cell loading with Rhodamine 123 and inhibition of Pgp-mediated Rhodamine 123 efflux assay

The capability of the compounds to inhibit Rhodamine 123 (R123) efflux was determined as already described previously.[S7] Briefly, L5178 MDR1 cells ($2x10^6$ ml^{-1}) were resuspended in serum-free McCoy's 5A medium, and 0.5 ml aliquots of the cell suspension were distributed into Eppendorf centrifuge tubes. Compounds tested were added at different concentrations and samples were incubated for 10 min at room temperature. Then, R123 was added to the samples at a final concentration of $5x10^{-6}$ M R123 and the cells were incubated for 20 min at 37 °C. Thereafter, the cells were washed twice by centrifugation for 5 min at 2,000 g and resuspended in 0.5 ml phosphate-buffered saline (PBS). R123 retained by cells was quantified as fluorescence, using a Becton-Dickinson FACS Calibur flow cytometer (San Josè, CA, USA) equipped with an ultraviolet argon laser (excitation at 488 nm, emission at 530/30 and 585/42 nm band-pass filters). FACS analysis were gated to include only individual, viable cells on the basis of forward and side light-scatter and were based on acquisition of data from 10,000 cells. Fluorescence signals were analyzed by the BDIS CellQuest software (Becton Dickinson, San Josè, CA, USA). The mean fluorescence intensity (MFI) was used for comparison among different conditions. Cyclosporine A

(CSA) was selected as the positive control for a standard inhibitor since already at $5x10^{-3}$ M concentration it can maximally inactivate the Pgp efflux pump.[S7,S8]

2.3 Data analysis and statistics

The percent Pgp inhibition exerted by a single compound was calculated as described previously.[S7,S8]

3. In Silico methods

3.1 VolSurf+

The latest version of Volsurf+ was used (1.0.4). All user settings were left at their default values, including the 'as is' import option. A PCA was created using all the descriptors available in the program. The first two-components of the PCA model were used.[S9]

3.2 GRID

The latest version of GRID was used (22c). The probes DRY, N1, and O were employed, with grid spacing set to 0.5 Å. All other settings were left at their default values for the calculation of the fields. DRY fields were depicted at -0.5 kcal mol^{-1}, while N1 and O fields were depicted at -3.5 kcal mol^{-1}.[S10]

Table S6. References

(S1) Kaatz, G. W.; Seo, S. M. Mechanisms of Fluoroquinolone Resistance in Genetically Related Strains of *Staphylococcus aureus*. *Antimicrob. Agents Chemother.* **1997,** *41,* 2733-2737.

(S2) Price, C. T. D.; Kaatz, G. W.; Gustafson, J. E. The multidrug efflux pump NorA is not required for salicylate-induced reduction in drug accumulation by *Staphylococcus aureus*. *Int. J. Antimicrob. Agents* **2002,** *20,* 206-213.

(S3) Clinical Laboratory Standards Institute. Methods for dilution antimicrobial susceptibility tests for bacteria that grow aerobically. Approved standard M7-A7, 7th ed.; Clinical and Laboratory Standards Institute: Wayne PA, 2006.

(S4) Eliopoulos, G. M.; Moellering, R. C. J. Antimicrobial combinations. In *Antibiotics in Laboratory Medicine*; Lorian, V. Ed.; Williams and Wilkins: Baltimore, MD, 1991; pp 432-492.

(S5) Kaatz, G. W.; Seo, S. M.; O'Brien, L.; Wahiduzzaman, M.; Foster, T. J. Evidence for the existence of a multidrug efflux transporter distinct from *norA* in *Staphylococcus aureus*. *Antimicrob. Agents Chemother.* **2000,** *44,* 1404-1406.

(S6) Weaver, J.L.; Szabo, G.Jr; Pine, P.S.; Gottesman, M.M.; Goldenberg, S.; Aszalos, A. The effect of ion channel blockers, immunosuppressive agents, and other drugs on the activity of the multi-drug transporter. *Int. J. Cancer* **1993**, *54,* 456-461.

(S7) Neri, A.; Frosini, M.; Valoti, M.; Cacace, M.G.; Teodori, E.; Sgaragli, G. N,N-Bis(cyclohexanol)amine aryl esters inhibit P-glycoprotein as transport substrates. *Biochem. Pharmacol.* **2011,** *82,* 1822-31.

(S8) Wang, E.J.; Casciano, C.N.; Clement, R.P.; Johnson, W.W. In vitro flow cytometry method to quantitatively assess inhibitors of P-glycoprotein. *Drug Metab. Dispos.* **2000**, *28,* 522-528.

(S9) Volsurf+ (version 1.0.4) is distributed by Molecular Discovery: http://www.moldiscovery.com/soft_vsplus.php

(S10) GRID (version 22c) is distributed by Molecular Discovery http://www.moldiscovery.com/soft_grid.php

Table S7. Purity of Active Compounds

Analysis. The purity of the active compounds was assessed by LC−MS according to the UV trace at 230 and 254 nm. Analytical LC−MS was run on the column Agilent Poroshell 120 EC-C18, 2.7 μm, 2.1x100mm. Gradient was from CH_3CN/H_2O (5:95) to 85% CH_3CN over 5 min. Flow was 0.3 mL/min. The LC−MS machines consisted of an HPLC Agilent 1290 Infinity System equipped with a MS detector Agilent 6540UHD Accurate Mass Q-TOF.

^{1}H NMR spectra were recorded at 400 with a Bruker Advance-DRX 400 instrument and with Me_4Si as the internal standard. The chemical shift (δ) values are reported in ppm, and the coupling constants (J) are given in Hz. The abbreviations used are as follows: s, singlet; bs, broad singlet; d, doublet; dd, double doublet; t, triplet; m, multiplet. The spectral data are consistent with the assigned structures.

Table S9. Data confirming the structure and the purity for active compounds (LC-MS and ^{1}H-NMR).

Compd.: 2 (Amlodipine besylate) **Vendor:** SIGMA **Vendor Code:** A5605

Name: 2-[(2-Aminoethoxy)-methyl]-4-(2-chlorophenyl)-1,4-dihydro-6-methyl-3,5-pyridinedicarboxylic acid 3-ethyl 5-methyl ester benzene sulfonate

Structure:

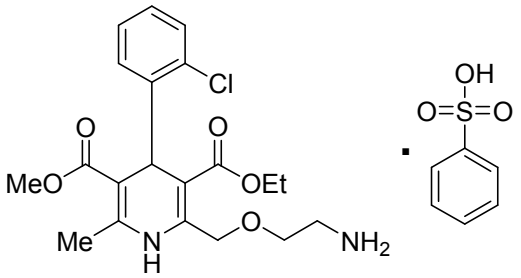

Formula: $C_{20}H_{25}ClN_2O_5$**.**$C_6H_6O_3S$ **MW:** 408,88+158,18

^{1}H-NMR: ($CDCl_3$ 400 MHz) δ 8.05 (bs, 3H), 7.88-7.85 (m, 2H), 7.48 (bs, 1H), 7.46-7.39 (m, 3H), 7.30 (dd, *J* = 7.67 and 1.80 Hz, 1H), 7.21 (dd, *J* = 7.88 and 1.44 Hz, 1H), 7.07 (dt, *J* = 7.37 and 1.43 Hz, 1H), 7.01 (dt, *J* = 7.32 and 1.77 Hz, 1H), 5.35 (s, 1H), 4.72 (d, *J* = 15.02 Hz, 1H), 4.61 (d, *J* = 15.00 Hz, 1H), 4.09-4.00 (m, 2H), 3.67-3.62 (m, 2H), 3.57 (s, 3H), 3.12-3.07 (m, 2H), 2.11 (s, 3H), 1.18 (t, *J* = 7.13 Hz, 3H).

Purity: >99%

LC-MS: t_R = 3.83 min. **MS (ESI):** *m/z* 409.152 $(M + H)^+$

Compd.: 3 (Astemizole) **Vendor:** SIGMA **Vendor Code:** A2861

Name: 1-(4-Fluorobenzyl)-2-(1-[4-methoxyphenethyl]piperidin-4-yl)aminobenzimidazole

Structure:

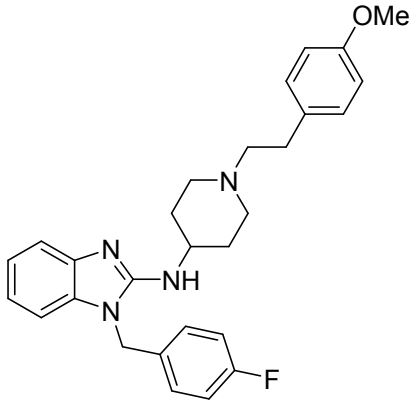

Formula: $C_{28}H_{31}FN_4O$ **MW:** 458,57

^{1}H-NMR: ($CDCl_3$ 400 MHz) δ 7.54 (dd, *J* = 7.81 and 0.71 Hz, 1H), 7.18-7.03 (m, 9H), 6.84 (d, *J* = 8.68 Hz, 2H), 5.07 (s, 2H), 4.03-3.95 (m, 1H), 3.80 (s, 3H), 3.73 (d, *J* = 8.03 Hz, 1H), 2.83-2.71 (m, 4H), 2.56-2.52 (m, 2H), 2.25 (t, *J* = 11.01 Hz, 2H), 2.14-2.10 (m, 2H), 1.48-1.38 (m, 2H).

Purity: >99%

LC-MS: t_R = 3.09 min. **MS (ESI):** *m/z* 459.256 $(M + H)^+$

Compd.: 4 (Dipyridamole) **Vendor:** SIGMA **Vendor Code:** D9766

Name: 2,2',2",2"'-(4,8-di(piperidin-1-yl)pyrimido[5,4-d]pyrimidine-2,6-diyl)bis(azanetriyl)tetraethanol

Structure:

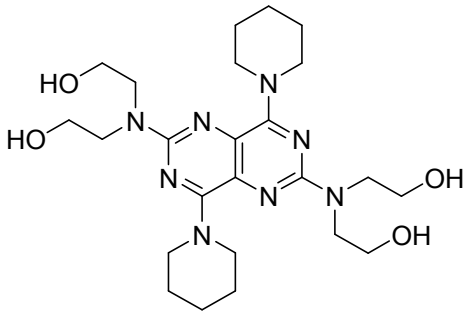

Formula: $C_{24}H_{40}N_8O_4$ **MW:** 504,63

^{1}H-NMR: ($CDCl_3$ 400 MHz) δ 4.35 (s, 8H), 4.30-3.20 (m, 28H), 1.71 (s, 12H),

Purity: >99%

LC-MS: t_R = 3.42 min. **MS (ESI):** *m/z* 505.327 $(M + H)^+$

Compd.: 5 (Loperamide hydrochloride) **Vendor:** SIGMA **Vendor Code:** L4762

Name: 4-(*p*-Chlorophenyl)-4-hydroxy-*N,N*-dimethyl-α,α-diphenyl-1-piperidinebutyramide hydrochloride

Structure:

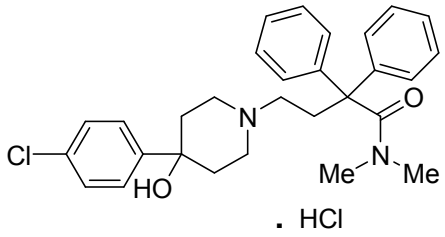

Formula: $C_{29}H_{33}ClN_2O_2$**.**HCl **MW:** 476,22+36.46

^{1}H-NMR: ($CDCl_3$ 400 MHz) δ 11.69 (bs, 1H), 7.45-7.26 (m, 14H), 3.32-3.12 (m, 4H), 2.95 (s, 3H), 2.88-2.68 (m, 7H), 2.29 (s, 3H), 1.78 (d, *J* = 13.95 Hz, 2H).

Purity: >99 %

LC-MS: t_R = 4.38 min. **MS (ESI):** *m/z* 477.234 $(M + H)^+$

Compd.: 6 (Quinidine) **Vendor:** SIGMA **Vendor Code:** Q3625

Name: (9*S*)-6'-(methyloxy)cinchonan-9-ol

Structure:

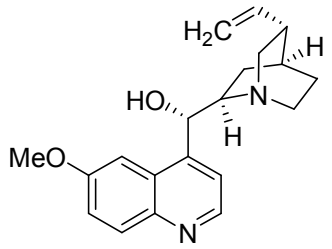

Formula: $C_{20}H_{24}N_2O_2$ **MW:** 324,42

^{1}H-NMR: ($CDCl_3$ 400 MHz) δ 8.59 (d, *J* = 4.54 Hz, 1H), 7.95 (d, *J* = 9.21 Hz, 1H), 7.50 (d, *J* = 4.51 Hz, 1H), 7.30 (dd, *J* = 9.22 and 2.70Hz, 1H), 7.19 (d, *J* = 2.67 Hz, 1H), 6.06-5.98 (m, 1H), 5.55 (d, *J* = 4.49 Hz, 1H), 5.05 (s, 1H), 5.02 (d, *J* = 5.38 Hz, 1H), 4.17 (bs, 1H), 3.87 (s, 3H), 3.28-3.23 (m, 1H), 3.08-3.04 (m, 1H), 2.92-2.73 (m, 3H), 2.22 (q, *J* = 8.89 Hz, 1H), 2.05-2.01 (m, 1H), 1.75 (s, 1H), 1.54-1.51 (m, 2H), 1.19-1.16 (m, 1H).

Purity: 93% + 7% dihydroquinidine (declared from supplier < 20% dihydroquinidine)

LC-MS: t_R = 2.22 min. MS (ESI): *m/z* 325.192 $(M + H)^+$

Compd.: 25 **Vendor:** Specs **Vendor Code:** AE-848/11245742

Name: *N*-(1-benzyl-2-methyl-1*H*-benzo[*d*]imidazol-5-yl)-4-methylbenzenesulfonamide

Structure:

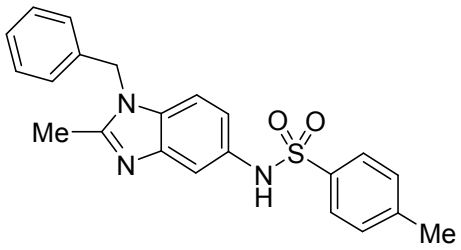

Formula: $C_{22}H_{21}N_3O_2S$ MW: 391,49

^{1}H-NMR: ($CDCl_3$ 400 MHz) δ 7.60 (d, *J* = 8.30 Hz, 2H), 7.33-7.29 (m, 4H), 7.23 (d, *J* = 1.81 Hz, 1H), 7.19 (d, *J* = 8.55 Hz, 2H), 7.13 (d, *J* = 8.57 Hz, 1H), 7.08 (dd, *J* = 8.58 and 1.95 Hz, 1H), 7.05-7.02 (m, 2H), 5.28 (s, 2H), 2.54 (s, 3H) , 2.46 (s, 3H).

Purity: >99 %

LC-MS: t_R = 3.73 min. MS (ESI): *m/z* 392.145 $(M + H)^+$

Compd.: 31 **Vendor:** KeyOrganics Vendor Code: SS-0082

Name: 2-((6-chloropyridin-3-yl)methylthio)-4-(trifluoromethyl)-5,6,7,8-tetrahydroquinoline-3-carbonitrile

Structure:

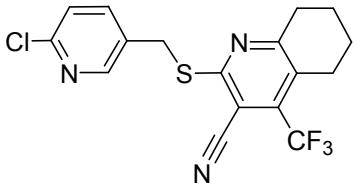

Formula: $C_{17}H_{13}ClF_3N_3S$ **MW:** 383,82

^{1}H-NMR: ($CDCl_3$ 400 MHz) δ 8.49 (d, *J* = 2.12 Hz, 1H), 7.74 (dd, *J* = 8.25 and 2.52 Hz, 1H), 7.28 (d, *J* = 8.42 Hz, 1H), 4.39 (s, 2H), 3.04 (t, *J* = 6.4 Hz, 2H), 2.89-2.86 (m, 2H), 1.94-1.88 (m, 2H), 1.86-1.80 (m, 2H).

Purity: >99%

LC-MS: t_R = 6.69 min. MS (ESI): *m/z* 384.061 $(M + H)^+$